

THE LUMINOSITY AND STELLAR MASS FUNCTIONS OF GRB HOST GALAXIES: INSIGHT INTO THE METALLICITY BIAS

MICHELE TRENTI^{1,2,†}, ROSALBA PERNA³, RAUL JIMENEZ^{4,5}*Draft version January 28, 2015*

ABSTRACT

Long-Duration Gamma-Ray Bursts (GRBs) are powerful probes of the star formation history of the Universe, but the correlation between the two depends on the highly debated presence and strength of a metallicity bias. To investigate this correlation, we use a phenomenological model that successfully describes star formation rates, luminosities and stellar masses of star forming galaxies, and apply it to GRB production. We predict the luminosities, stellar masses, and metallicities of host galaxies depending on the presence (or absence) of a metallicity bias. Our best fitting model includes a moderate metallicity bias, broadly consistent with the large majority of the long-duration GRBs in metal-poor environments originating from a collapsar (probability $\sim 83\%$, with $[0.74; 0.91]$ range at 90% confidence level), but with a secondary contribution ($\sim 17\%$) from a metal-independent production channel, such as binary evolution. Because of the mass-metallicity relation of galaxies, the maximum likelihood model predicts that the metal-independent channel becomes dominant at $z \lesssim 2$, where hosts have higher metallicities and collapsars are suppressed. This possibly explains why some studies find no clear evidence of a metal-bias based on low- z samples. However, while metallicity predictions match observations well at high redshift ($z \gtrsim 2$), there is tension with low redshift observations, since a significant fraction of GRB hosts are predicted to have (near) solar metallicity. This is in contrast to observations, unless obscured, metal-rich hosts are preferentially missed in current datasets, and suggests that lower efficiencies of the metal-independent GRB channel might be preferred following a comprehensive fit that includes metallicity of GRB hosts from *complete* samples. Overall, we are able to clearly establish the presence of a metallicity bias for GRB production, but continued characterization of GRB host galaxies is needed to quantify its strength. Tabulated model predictions are available in electronic format.

Subject headings: galaxies: high-redshift — galaxies: general — gamma-ray burst: general — stars: formation

1. INTRODUCTION

Long-duration ($t \gtrsim 2$ s) Gamma Ray Bursts, simply indicated as GRBs throughout this paper, are widely considered powerful tracers of the star formation history of the Universe (Bloom et al. 2002; Chary et al. 2007; Savaglio et al. 2009; Robertson & Ellis 2012). In fact, their progenitors are established to be short-lived, massive stars (Galama et al. 1998; Hjorth et al. 2003; Woosley & Heger 2006; Berger et al. 2011) and the GRBs and their afterglows are sufficiently luminous to be detected as early as ~ 500 Myr after the Big Bang ($z \sim 9.4$, see Salvaterra et al. 2009; Tanvir et al. 2009; Cucchiara et al. 2011). Furthermore, the detectability of GRBs is not limited by how faint their host galaxies might be, making them potential tracers of the *total* star formation rate at high-redshift, unlike surveys of Lyman-Break Galaxies (LBGs), which trace star formation only in systems above the survey detection limit (Trenti et al. 2013). This advantage of GRBs over LBGs as star formation tracers is highlighted by the non-detection of the majority of GRB host galaxies at $z \gtrsim 5$, which indicates that even the deepest observations of LBGs with the Hubble Space Telescope (HST) are

only capturing the tip of the iceberg of star formation during the first billion years after the Big Bang (Trenti et al. 2012; Tanvir et al. 2012).

However, the use of GRBs as star formation tracers presents significant challenges as well. First, the sample size of GRBs at high- z is still very small, introducing significant Poisson noise. For example, there are only ~ 40 GRBs at $z \gtrsim 3.5$ and a handful at $z > 6.5^7$, whereas more than 11000 LBGs have been identified at $z \gtrsim 3.5$, and more than 800 at $z \gtrsim 6.5$ (Bouwens et al. 2014b). Second, several studies suggest that the connection between GRB rate and star formation rate is likely biased by the metallicity of the GRB progenitor, with low-metallicity environments having a higher yield of GRBs.

The presence of a metallicity bias has both observational and theoretical support: Several groups found that host galaxies of GRBs appear to lie below the typical mass-metallicity relation observed for star-forming galaxies (Fynbo et al. 2003; Prochaska et al. 2004; Modjaz et al. 2006; Fruchter et al. 2006; Thoene et al. 2007; Graham & Fruchter 2012; Wang & Dai 2014), and this result fits well within the leading theoretical framework for GRB engine, the *collapsar* model (Woosley 1993; MacFadyen & Woosley 1999). According to this model, the GRB progenitor is a massive star whose rapidly rotating core collapses to form a black hole, while the outer envelope falls back and forms an hyperaccreting disk (if endowed with sufficient angular momentum), powering an energetic relativistic jet. Since stellar mass losses grow with increasing metallicity, and carry away precious angular momentum from the star, an enhancement of

mtrenti@unimelb.edu.au

¹ Institute of Astronomy and Kavli Institute for Cosmology, University of Cambridge, Madingley Road, Cambridge, CB3 0HA, United Kingdom² School of Physics, The University of Melbourne, VIC 3010, Australia³ Department of Physics and Astronomy, Stony Brook University, Stony Brook, NY 11794-3800, USA⁴ ICREA & ICC, University of Barcelona, Martí i Franques 1, 08028 Barcelona, Spain⁵ Institute for Applied Computational Science, Harvard University, MA 02138, USA[†] Kavli Institute Fellow⁷ http://swift.gsfc.nasa.gov/archive/grb_table/

the GRB rate in low-metallicity environments is expected (Woosley & Heger 2006; Yoon et al. 2006; Nuze et al. 2007; Perna et al. 2014), possibly with a sharp cut-off around solar metallicity (Stanek et al. 2006; Yoon et al. 2006). However, this scenario for GRB production is at odds with other observational findings of GRB host galaxies that have solar or even super-solar metallicity (Berger et al. 2007; Levesque et al. 2010c; Savaglio et al. 2012), and alternative models to the *collapsar* scenario have been proposed, such as progenitors in binaries (Fryer & Heger 2005; Cantiello et al. 2007), which are less influenced by metallicity.

Such a complex mix of observational and theoretical results on the presence, and strength, of a metallicity bias arguably represents the most significant limiting factor in the use of GRBs as reliable tracers of star formation (Stanek et al. 2006; Kewley et al. 2007; Modjaz et al. 2008; Jimenez & Piran 2013, but see the recent paper by Hunt et al. 2014). A deeper, and clearer, understanding of how metallicity influences the relation between GRB and star formation rate is needed to be able to account and correct for the bias. In this respect, there are two separate questions to address:

- Are GRBs more probable in low-metallicity environments compared to higher metallicity ones?
- Is there a maximum metallicity cut-off?

Both affect the connection between GRB and star formation, with an impact that in general varies over redshift, reflecting the evolution in the chemical enrichment of galaxies throughout cosmic history.

GRB host galaxy studies are an ideal tool to understand if a metallicity bias is present, and how strong it is. As such, they have been the subject of extensive studies (we refer the reader to the comprehensive review by Levesque 2014), but no clear consensus has been reached in the community. Some investigations point toward a clear presence of a metallicity-dependence in the production of GRBs (e.g., Boissier et al. 2013; Lunnan et al. 2014), while others conclude that GRBs appear to be unbiased tracers of star formation (e.g., Fynbo et al. 2008; Kohn et al. 2015), and some highlight that discrimination between scenarios is challenging (e.g., Pontzen et al. 2010; Laskar et al. 2011).

Ideally, spectroscopic samples are the most suited for the task of quantifying the bias, since they allow to establish a direct connection between GRBs and host metallicity. However, measuring the metallicity of galaxies at high redshift is challenging, and generally limited only to the brightest objects. A wider study extending to fainter hosts is possible by characterizing luminosities and stellar masses of GRB host galaxies from broad-band photometry, and then comparing sample properties against those of LBGs. Qualitatively, a GRB preference for low-metallicity environments is reflected into steeper luminosity and mass functions at the faint end compared to a scenario without bias, because of the established existence of a mass/luminosity vs. metallicity relation (Panter, Heavens, & Jimenez 2003; Panter et al. 2008; Maiolino et al. 2008; Mannucci et al. 2010). Similarly, the presence of a metallicity cutoff would introduce a truncation of the luminosity/mass function for the brightest and most massive hosts.

Even in absence of a metallicity bias, the luminosity and mass functions of GRB hosts differ from those of LBGs because the GRB rate is proportional to the star formation rate (SFR), making the host skewed toward inclusion of systems

with higher SFR (i.e. luminosity), hence resulting in a shallower luminosity function. If $\phi_{\text{LBG}}(L)$ is the luminosity function of LBGs, then under the basic assumption that the luminosity density and the star formation rates are proportional and that there is no metallicity bias, it follows that the GRB host luminosity function is proportional to $\phi_{\text{LBG}}(L) \times L$. There is, though, one second order but subtle and crucial correction that needs to be made to this relation to properly quantify how any deviation from it is connected to the metallicity bias. That is proper modeling of dust⁸. In fact, the GRB rate depends on the intrinsic star formation rate, hence on the intrinsic luminosity, not on the observed one. As a result, the scaling for the GRB luminosity function (again with no bias) goes as $\phi_{\text{GRB}}(L_{\text{obs}}) \propto \phi_{\text{LBG}}(L_{\text{obs}}) \times L_{\text{int}}$. Since $L_{\text{int}}/L_{\text{obs}}$ depends on the metallicity (higher dust content is typically associated with higher metallicity environments), this effect may partially mask the presence of a metallicity bias, unless proper dust treatment is taken into account in the data-model comparison.

Finally, it is also important to recall that, since all the proposed GRB engines are generically associated with the death of massive stars, it is generally expected that studies which focus on luminosity functions at wavelengths that are good tracers of *recent* star formation are those most suited for the purpose of understanding the connection between GRBs and star formation. In this respect, the two most natural choices are UV or far-IR. In this work, we focus on the first, motivated primarily by the availability of high quality UV luminosity functions for LBGs. To present a comprehensive analysis, we include stellar mass functions in the modeling, but the latter are not as powerful because the connection between star formation and stellar mass is not as tight as it is with UV luminosity. For example, the most massive elliptical galaxies in the local universe have little to no recent star formation, making them highly unlikely to host GRBs.

To complement and augment the previous studies of the metallicity bias of GRB host galaxies, we take a novel approach, starting from a successful modeling framework that we developed to investigate how the luminosity function of LBGs evolves with redshift and how it is connected to the underlying dark matter halo mass function. In Trenti et al. (2010) we constructed a first link between luminosity and dark matter halo mass functions, quantitatively predicting the LBG luminosity function during the epoch of reionization. In particular, the model predicted an accelerated decrease of the luminosity density of galaxies at $z \gtrsim 8$ and a steepening of the faint-end slope of the luminosity function, with both predictions recently verified thanks to the array of new Hubble observations of $z \gtrsim 8$ galaxies (Bradley et al. 2012; Schmidt et al. 2014; Ellis et al. 2013; McLure, et al. 2013; Bouwens et al. 2014b). We also applied our luminosity function model to interpret the non-detections of GRB host galaxies at $z > 5$ by Tanvir et al. (2012), concluding (see Trenti et al. 2012) that the majority of star formation at $z > 6$ is happening in faint systems below the current detection limit (a conclusion deriving naturally from the luminosity function steepening; see also Salvaterra et al. 2013 which supports earlier results). More recently, we extended our modeling to achieve a comprehensive description of the LBG UV luminosity function evolution from $z \sim 0$ to $z \sim 10$, capturing at the same time the stellar mass density and specific star formation

⁸ For some discussion on the influence of dust on deriving physical properties of galaxies from their stellar populations see e.g. Tojeiro et al. (2007)

rate evolution (Tacchella, Trenti & Carollo 2013). We hence applied the model to investigate the connection between GRB rate and star formation rate and how it varies with redshift and with the presence of a metallicity bias (Trenti et al. 2013). Our key conclusions were: (1) the best model for the GRB rate is one that includes production at low metallicity primarily through the collapsar engine ($\sim 75\text{--}80\%$), with metallicity bias, combined with a second, metal-independent channel ($\sim 20\text{--}25\%$), such as a progenitor star in a binary system; and (2) the metallicity bias becomes negligible to first approximation at $z \gtrsim 4$, since the majority of star forming galaxies have low metallicity $Z \lesssim 0.1Z_\odot$. While the conclusions reached were interesting and shed some new light on the problem, our study was limited by the uncertainty in the comoving GRB rate.

In this work, we aim at building upon our previous framework to expand the data-model comparison to UV luminosity functions, stellar mass functions, and metallicities of GRB hosts, with the goal of providing a more stringent and rigorous characterization of the metallicity bias. We extend our previous modeling by taking into account other effects, such as dust obscuration, that are likely to influence the data-model comparison. In addition, by presenting predictions for the redshift evolution of GRB hosts luminosity and stellar mass function, we make testable predictions that can guide the design of the next generation of surveys aimed at characterizing their properties. The paper is organized as follows. Section 2 describes our model, whose results are presented in Section 3, and then compared to the current observations in Section 4. Section 5 summarizes and concludes with an outlook for the future.

Throughout the paper we use the latest Λ CDM concordance cosmological model with parameters determined by the *Planck* mission: $\Omega_{\Lambda,0} = 0.685$, $\Omega_{m,0} = 0.315$, $\Omega_{b,0} = 0.0462$, $\sigma_8 = 0.828$, $n_s = 0.9585$, $h = 0.673$ (Planck Collaboration 2013).

2. MODELING: GRB RATE AND HOST GALAXY PROPERTIES

Following the framework developed in Trenti et al. (2013), we base our modeling on linking star formation to the assembly of dark-matter halos. We assume that each halo converts a fraction of its total mass $\xi(M_h)$ into stars ($M_* = \xi(M_h) \times M_h$) with a constant star formation rate over the timescale defined by the halo-assembly time $t_{1/2}(M_h, z)$, that is the time needed to grow from $M_h/2$ to M_h . $\xi(M_h)$ depends on mass but not on redshift (Tacchella, Trenti & Carollo 2013; Behroozi et al. 2013), while $t_{1/2}$ decreases both for increasing mass and redshift (e.g., see Lacey & Cole 1993). The UV luminosity of the galaxies in our model is computed via Stellar Population models, assuming a Salpeter initial mass function from $0.1 M_\odot$ to $100 M_\odot$ (Bruzual & Charlot 2003). At fixed halo (and stellar) mass, higher z halos form stars on a shorter timescale, hence they have higher UV luminosity (see Tacchella, Trenti & Carollo 2013; Trenti et al. 2013 for further details).

The star formation efficiency $\xi(M_h)$ is calibrated at one reference redshift, thanks to abundance matching between the galaxy luminosity function and the dark-matter halo mass function. After such calibration, the model has no free parameters, and the evolution of the dark-matter halo mass function and of the halo assembly time fully determines the star formation rate and galaxy luminosity function at all other redshifts. As discussed in Tacchella, Trenti & Carollo (2013), this minimal model with no free parameters is remarkably successful in capturing the evolution from $z \sim 0$

to $z \sim 10$ of (1) the UV luminosity density (star formation rate); (2) the galaxy luminosity function; and (3) the stellar mass density and specific star formation rate. Like in our previous work, we calibrate $\xi(M_h)$ at $z = 4$. Here, we use the Sheth & Tormen (1999) halo mass function and the latest determination of the observed UV luminosity function [$\phi(L) = \phi^*(L/L^*)^\alpha \exp(-(L/L^*))$] derived by Bouwens et al. (2014b): $\phi^* = 1.35^{+0.22}_{-0.19} \times 10^{-3} \text{ Mpc}^{-3}$; $\alpha = -1.65 \pm 0.03$ and $M_{AB}^{(*)} = -21.08$, where $M^{(*)} = -2.5 \log_{10} L^*$. We assume that the LF extends to fainter than observed luminosity, down to $M_{UV} \leq -11$, which corresponds to $M_h \gtrsim 5 \times 10^8 M_\odot$ at $z \sim 4$ (e.g. see Trenti et al. 2010; Tacchella, Trenti & Carollo 2013). While this represents a significant extrapolation compared to the typical magnitude limit of Lyman-Break galaxy surveys ($M_{UV} \sim -17$, see Bouwens et al. 2007), observations of LBGs behind gravitational lenses have shown that the LF of LBGs at $z \sim 2$ continues to be a steep power law at $M_{UV} \sim -13$ (Alavi et al. 2013). Note that star forming sites with UV magnitude above $M_{AB} > -11$ are unlikely to host a GRB in any case, since their star formation rate is so low ($\dot{\rho}_* \lesssim 1.3 \times 10^{-3} M_\odot \text{ yr}^{-1}$) that stochastic sampling of the IMF is not expected to lead to the formation of any star with $M \gtrsim 30 M_\odot$ within the typical dynamical time of a molecular cloud ($t_{dyn} \sim 10^4 \text{ yr}$).

Since the observed UV luminosity is significantly affected by dust extinction, we include in our modeling dust extinction with an empirically calibrated formula following Bouwens et al. (2014a) and Meurer et al. (1999), which link extinction to the UV-continuum slope β (for a spectrum modeled as $f_\lambda \sim \lambda^\beta$): $A_{UV} = 4.43 + 1.99\beta$. We model the observations by Bouwens et al. (2014a) as:

$$\begin{aligned} <\beta(z, M_{AB})> = \\ \begin{cases} a(z) \exp(b(z)M_{AB}) + c & \text{if } M_{AB} \geq M_0 \\ c - a(z) \exp(b(z)M_0)(-1 + b(z)(M_0 - M_{AB})) & \text{if } M_{AB} < M_0 \end{cases} \end{aligned} \quad (1)$$

where $c = -2.276$, $M_0 = -22$ and $a(z)$, $b(z)$ are determined from fitting the Bouwens et al. (2014a) measurements. Assuming (like in Tacchella, Trenti & Carollo 2013) a Gaussian distribution for β at each M_{UV} value with dispersion $\sigma_\beta = 0.34$, then the average extinction $<A_{UV}>$ is given by:

$$<A_{M_{UV}}> = 4.43 + 0.79 \ln(10) \sigma_\beta^2 + 1.99 <\beta>. \quad (2)$$

This dust extinction framework differs slightly from the one we adopted earlier where we had a linear dependence for $\beta(M_{AB})$. In fact, the latest determination of β by Bouwens et al. (2014a) shows evidence for a curved relation between UV slope and absolute magnitude. We adopt empirically an exponential function, which provides a good fit, and then extrapolate it linearly, like in our previous work, at high luminosities ($M_{AB} < -22$, where there are only limited observations). The use of the exponential fit for faint magnitudes has the advantage of avoiding unphysical negative dust corrections.

To model the production of GRBs, we include a metallicity-dependent efficiency as in Trenti et al. (2013). Galaxies are assigned a metallicity dependence on redshift and luminosity following the relation derived by Maiolino et al. (2008), after we convert our UV luminosity in stellar mass. Specifically, we use their Equation (2) with coefficients given in their Table 5 for the Bruzual & Charlot (2003) spectral energy distribution template. Coefficients are linearly interpolated in redshift space among data points. At $z > 3.5$ we assume no further

evolution of the mass-metallicity relation. Since our model implies a one-to-one map of stellar mass to star formation rate at fixed redshift, with the assumption of a mass-metallicity relation we are also defining a metallicity-star-formation rate relation. In Section 3.4 we compare our model results to the fundamental relation derived by Mannucci et al. (2010) at $z < 2.5$.

The efficiency of GRB production versus metallicity Z is based on the idea that we expect two main contributions to long-duration GRB production. A channel broadly based on evolution of single massive stars, where metallicity plays a crucial role in regulating mass loss via winds (the Collapsar model, e.g. Yoon et al. 2006), plus alternative channels without strong metallicity dependence (e.g., for binary progenitors, Fryer & Heger 2005). Combining the output from the Yoon et al. (2006) Collapsar simulations with a metallicity-independent plateau, we write the total GRB efficiency $\kappa(Z)$ as:

$$\kappa(Z) = \kappa_0 \times \frac{a \log_{10} Z/Z_\odot + b + p}{1 + p}, \quad (3)$$

where κ_0 , p , a , and b take the same values as in Trenti et al. (2013): For $Z/Z_\odot \leq 10^{-3}$, $a = 0$, $b = 1$; for $10^{-3} \leq Z/Z_\odot \leq 10^{-1}$, $a = -3/8$, $b = -1/8$; for $10^{-1} \leq Z/Z_\odot \leq 1$, $a = -1/4$, $b = 0$; for $Z/Z_\odot > 1$, $a = 0$, $b = 0$. A fiducial value of $p = 0.2$ is used to construct our reference model. κ_0 is an overall normalization which has no impact on predictions for the luminosity functions of GRB hosts. The quantity $p/(1+p)$ can be interpreted as the probability that a GRB originates from the metal-independent channel rather than from a collapsar, *in the limit of metallicity of the host galaxy approaching zero*. We emphasize that p is *not* a relative probability but rather a minimum, metal-independent *plateau* value for the efficiency of forming GRBs. The relative probability of having GRBs originating from the two channels can only be computed after taking into account the metallicity distribution of the star forming galaxies, and this quantity generally strongly depends on the redshift because of the evolving mass-metallicity relation of galaxies (see Section 3 for a more detailed discussion).

To take into account both the intrinsic scatter in the mass-metallicity relation, as well as the likely presence of a spread in the metallicity of star forming gas within a given galaxy, we assume that Z follows a log-normal distribution, with $\langle \ln(Z) \rangle$ given by the mass-metallicity relation and $\sigma = 0.4$. This value corresponds to about 0.15 dex of intrinsic scatter in $\log_{10}(Z)$ (e.g., see Panter et al. 2008) and gives the resulting $\langle \kappa(Z) \rangle$ shown in Figure 1. We calculate the comoving GRB rate from the model star formation rate, weighted by $\langle \kappa(Z) \rangle$.

To demonstrate that our framework is successful in describing the evolution of the properties of the LBG population, we compare model predictions for the star formation rate (luminosity density) and stellar mass density to observations in Fig. 2. Further model validation and discussion of the comparison with observations of the LBG luminosity functions and specific star formation rates from $z \sim 0.3$ to $z \sim 8$ can be found in Tacchella, Trenti & Carollo (2013).

To derive predictions for the UV LF of GRB host galaxies, we start from the dust-attenuated (observed) LF of LBGs $\phi_{\text{LBG}}(L_{\text{obs}})$, and apply a weighting to the LF which takes into account the fact that the galaxies are selected based on the presence of a GRB. First, since the GRB rate is proportional to the star formation rate, more luminous host galaxies are preferentially present in a sample of observations targeted at GRB locations. Second, the metallicity bias must also be accounted

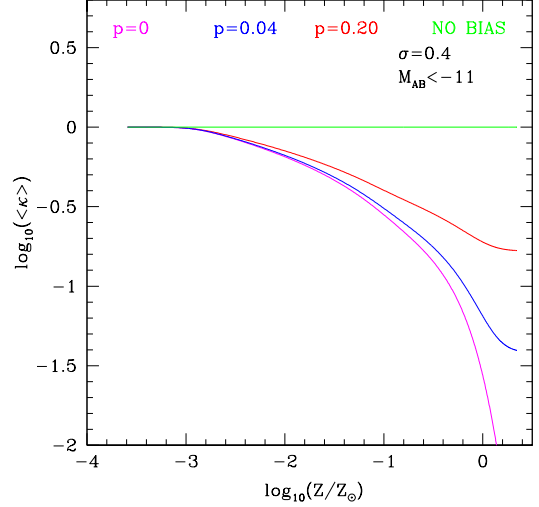


FIG. 1.— Efficiency of GRB production per unit stellar mass as a function of host-galaxy metallicity for different values of the metal-independent plateau parameter p , from $p = 0$ (magenta) to $p = +\infty$ (green).

for, introducing a further weight by $\langle \kappa(Z(M_{\text{AB}})) \rangle$. When introducing these weights, it is crucial to note that the GRB rate is proportional to the intrinsic star formation rate and not to the observed (dust-attenuated) one, therefore the correct weight to use is $L_{\text{int}} = 10^{-M_{\text{AB}}^{(\text{int})}/2.5}$, where $M_{\text{AB}}^{(\text{int})} = M_{\text{AB}}^{(\text{obs})} - A_{\text{UV}}(M_{\text{AB}}^{(\text{obs})})$. Hence we can write:

$$\phi_{\text{GRBhost}}(L_{\text{obs}}) \propto \phi_{\text{LBG}}(L_{\text{obs}}) \times L_{\text{int}} \times \langle \kappa(Z) \rangle, \quad (4)$$

which can be rewritten as:

$$\phi_{\text{GRBhost}}(L_{\text{obs}}) \propto \phi_{\text{LBG}}(L_{\text{obs}}) \times L_{\text{obs}} \times 10^{A_{\text{UV}}(M_{\text{AB}}^{(\text{obs})})/2.5} \times \langle \kappa(Z) \rangle. \quad (5)$$

Similarly, we proceed to construct predictions for the stellar mass function of GRB hosts, and for their metallicity distribution.

3. MODELING RESULT

3.1. Comoving GRB rate

The comoving GRB rate predicted by our model is shown in Figure 3, and compared to the observed event rate as derived by Wanderman & Piran (2010). Since the rate encompasses information from the full sample of GRBs, it provides the most stringent constraints on the free parameter of our model, the metallicity plateau p . Thus we use the inference from the GRB rate to construct a canonical model, and then we test its predictions against observations of GRB hosts luminosity/star formation rate and metallicities, which are available only for small sub-samples. As expected, the data-model comparison is similar to our previous analysis from Trenti et al. (2013). A small, but non-zero value of p provides the best description of the redshift evolution of the GRB rate. The highest likelihood when the rate is fitted at $z < 6$ is given by $p \sim 0.2$ (Figure 4), which we assume as our canonical model (red curve with shaded uncertainty region in Figure 3). Both lower and higher p exhibit systematic differences from the observations, implying that the comoving rate points toward the presence of a metallicity bias in GRBs, but that a non-zero fraction of events needs to originate from a metal-independent channel. This conclusion confirms the findings of Trenti et al. (2013), with a slightly revised quantitative result (the canonical model

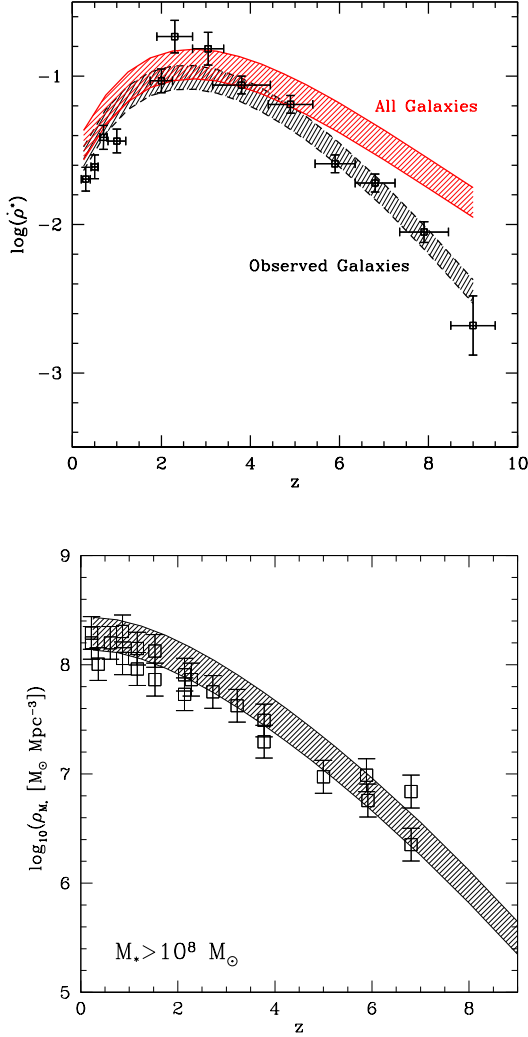


FIG. 2.— Left panel: Star formation rate versus redshift (black points), inferred from LBG observations in the UV integrated to $M_{AB} = -17.0$ including dust corrections (Bouwens et al. 2014a). Predictions from our LF model are shown as black shaded area when integrated to the same limiting magnitude as the data, highlighting the ability of our framework to describe the star formation history of the Universe. The red shaded region shows model predictions when integrated to $M_{AB} = -11.0$ (faintest galaxy assumed in the modeling). Right panel: Stellar mass density versus redshift for a compilation of observations from Tacchella, Trenti & Carollo (2013) (black data-points) and predictions from our model. Both data and model predictions for stellar mass density are integrated for $M_* > 10^8 M_\odot$.

considered in our earlier work had $p = 0.3$) arising because we updated the model calibration using the latest LBG luminosity function and dust content determinations by Bouwens et al. (2014a) and Bouwens et al. (2014b).

Figure 5 shows how the production of GRBs in our canonical model switches from predominantly Collapsars (metal-biased) at high-redshift, when most star forming sites have low metallicity, to metal-independent (binary evolution) as the redshift decreases. This happens because Collapsars are progressively suppressed by the increasing metallicity while the metal-independent channel continues to act unaffected, leading to an overall decrease with redshift of the efficiency of GRB production per unit stellar mass in star formation. By redshift $z = 0$ our canonical model with plateau $p = 0.2$ pre-

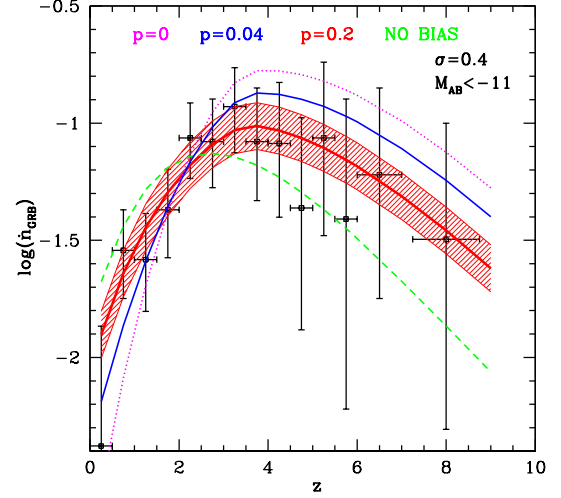


FIG. 3.— GRB comoving rate from Wanderman & Piran (2010), shown as black points with errorbars, compared to predictions of our models depending on the assumed efficiency of the metal-independent channel for GRBs. Our reference model ($p \sim 0.2$, shown in bold red with shaded region for typical model uncertainty) provides the best description of the data. Models with stronger metal bias are shown in magenta and blue, while a no-bias model is shown in green.

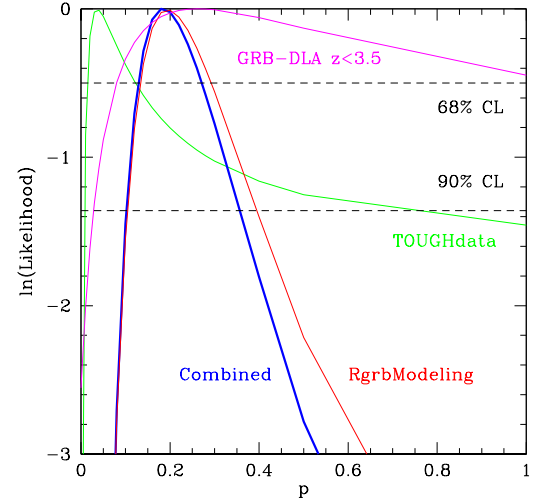


FIG. 4.— Likelihood for the value of the metal-independent channel for GRB production (p), derived from the comoving GRB rate (red line), from the star formation rates of the TOUGH survey (unbiased sub-sample, green line), from the metallicity of GRB-DLAs at $z < 3.5$ (magenta line, observations from Cucchiara et al. 2014), and combining the three constraints (blue line). Dashed horizontal lines denote the likelihood boundaries at 68% and 90% confidence. Because of the small sizes of the TOUGH unbiased sub-sample and of the GRB-DLA sample, the strongest constraint on p originates from comoving rate modeling.

dicts that over 90% of the GRBs are produced by the metal-independent channel (see Figure 5). If we assume instead a smaller value for p , for example $p = 0.04$ in Figure 5 (blue line), then we see that the relative fraction of Collapsars is higher. In this case Collapsars are still sub-dominant at $z = 0$, but they quickly become the major mode of GRB production at $z \gtrsim 1$, where the majority of observed GRBs are located.

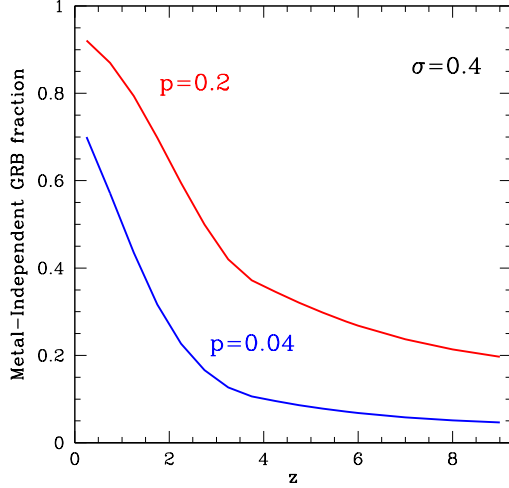


FIG. 5.— Fraction of GRB produced by the metal independent channel as a function of redshift for our model with $p = 0.2$ (solid red line), compared to the model with $p = 0.04$ (solid blue line). At low redshift the majority of GRBs in both models are produced by this channel, while at high- z the production approaches the asymptotic value $p/(1+p)$, and thus most GRBs are expected to originate from Collapsars.

Values of $p < 0.04$ further suppress the metal-independent channel, leading to a decrease of the rate of low- z GRBs, while Collapsars become the dominant progenitor channel at all redshifts.

3.2. UV luminosity functions and star formation rates

Using Equation (5) we construct the GRB-host galaxy luminosity function at different redshifts, and present the results in Figure 6. The best-fitting Schechter parameters $M_{AB}^{(*)}$ and α are reported in Table 1 in the magnitude range $-22.5 \leq M_{AB} \leq -17.0$. The full luminosity function model output is published in the electronic edition of the article, and Table 2 shows a portion for guidance regarding its form and content.

In general, we find that a Schechter LF provides a good description of the modeling output in the magnitude range considered, with typical values of $M_{AB}^{(*)}$ similar to those of the LBG LF at the same redshift, that is $-21.2 \lesssim M_{AB}^{(*)} \lesssim -19.4$, with higher values at low z . The faint-end slope α is also evolving with redshift, from $\alpha(z=0) \sim -0.1$ to $\alpha(z=9) \sim -1.4$. Translating the luminosity functions into the probability of detecting a GRB host galaxy as a function of the limiting magnitude of the observations, we predict that GRB host surveys reaching $M_{AB} = -18.0$ will have greater than 50% completeness at $z < 4$ (see bold red dotted line in Figure 8). Observations reaching significantly deeper, to $M_{AB} = -16.0$, are needed for the same completeness at $z > 7$, as a result of the steepening of the LF (see also Salvaterra et al. 2013 for independent modeling of the high- z hosts).

When compared to the model predictions for the LF of LBGs, we see that for most redshifts in our canonical case of $p = 0.2$, the GRB hosts empirically follow an approximate scaling with $\phi_{LBG}(L_{obs}) \times L_{obs}$ when a metallicity bias is present. This apparently counter-intuitive result is illustrated in more detail in Figure 7 and stems from the presence of dust absorption. In fact, Equation (5) shows that since dust and metallicity correlate, the effect of the metallicity bias is partially countered by the dust absorption term, present in

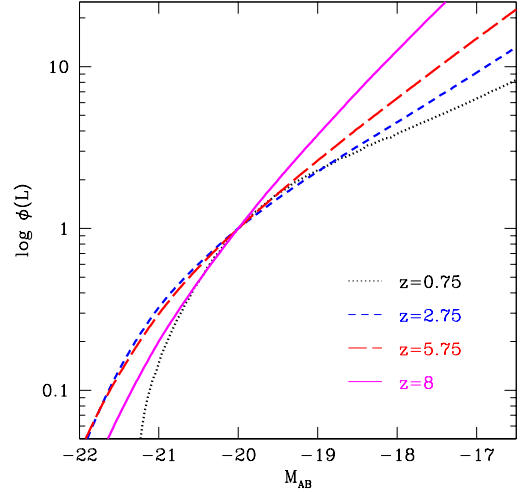


FIG. 6.— Predictions for the UV luminosity function of GRB host galaxies based on our reference model which includes a GRB metallicity bias for different redshifts. The best fitting Schechter parameters associated to the curves shown are given in Table 1. The curves have been normalized to have the same volume density at $M_{AB} = -20.0$. The plot shows that bright GRB host galaxies are rare both at low (black dotted, $z = 0.75$) and very high redshift (solid magenta, $z = 8$), respectively because of high metallicity (leading to both suppression of GRB production and significant reddening), and intrinsic rarity of massive, luminous galaxies at early times. Intermediate redshifts are shown as short dashed blue line ($z = 2.75$) and long-dashed red line ($z = 5.75$). As the redshift increases, the LF becomes steadily steeper at the faint end.

the equation because the GRB rate traces the intrinsic (dust-corrected) luminosity density. This is a key finding of our work: If one were to neglect the impact of dust and only consider the observed LF of LBG, then there would be the expectation that observing a GRB host luminosity function scaling as $\phi_{LBG}(L_{obs}) \times L_{obs}$ would mean that no metallicity bias is present.

Furthermore, because of the mass-metallicity relation of galaxies and of its redshift evolution, the impact of the metallicity bias on the LF shape depends strongly on the redshift. At very low redshift, a significant fraction of GRBs in the canonical model originates from the metal-independent channel, since GRB production by collapsar is suppressed in most hosts. In fact, the mass-metallicity relation we use in this work, which is based on Kewley & Ellison (2008) at $z \sim 0^9$, predicts $Z \geq Z_{\odot}$ (with Z_{\odot} corresponding to $12 + \log(O/H) = 8.7$) for a galaxy with stellar mass $\gtrsim 2 \times 10^9 M_{\odot}$ which has $M_{AB} \lesssim -17$ (after including dust extinction). Then, at an intermediate redshift, there is a transition to a regime where the effect of the metallicity bias is most pronounced in producing a steepening of the GRB host LF. Finally, at very high- z , the shape of the LF of GRBs is no longer affected by the metallicity bias since the majority of star forming sites have very low metallicities. At $z \gtrsim 5$ we thus predict that GRBs become essentially unbiased tracers of the star formation rate, since the majority of star forming sites have low metallicity and thus $\langle \kappa \rangle \rightarrow 1$ independent of the value of p (see Figure 1; see also

⁹ Our mass-metallicity relation at $z = 0.07$ derives from Kewley & Ellison (2008) with calibration done using the Kewley & Dopita (2002) method, and conversion of stellar masses to account self-consistently for the Bruzual & Charlot (2003) initial mass function. We recall we are simply implementing the relation by Maiolino et al. (2008), hence further details are available from that work (see, e.g. their Table 5 and Figure 7).

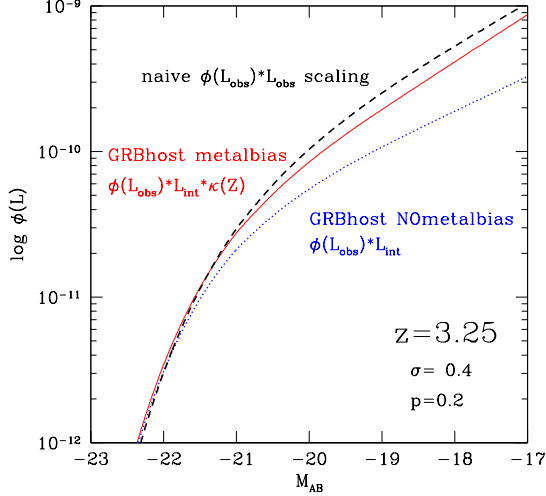


FIG. 7.— Illustration of the combined effect of dust reddening and metallicity bias in determining the shape of the GRB host galaxy LF at $z = 3.25$. The LF (red solid) is steepened by $\Delta\alpha \sim 0.2$ because of metallicity bias in GRB production compared to a model where the GRB rate traces the star formation rate (blue dotted). Still, because of the difference between intrinsic versus observed luminosity, L_{int} and L_{obs} , induced by reddening, the final GRB-host LF looks very similar to $\phi(L_{\text{obs}}) * L_{\text{obs}}$ shown as black long dashed line. Thus one could naively, but wrongly, infer that there is no metallicity bias!

Salvaterra et al. 2013).

In Figure 8 we show predictions for typical luminosities and star formation rates of GRB hosts for models with different p . If we set $p = 0$ in Eq. 3 (strong metallicity bias), GRBs cannot be hosted in galaxies with metallicity $Z \geq Z_{\odot}$, which introduces a sharp bright-end cut-off in the LF. This is evident by looking at the sharp decrease in all luminosity quantities at $z < 3$ for the $p = 0$ model (red lines in the top left panel of Figure 8). At higher redshift, a suppression of the host LF at the bright end is still present, but hardly distinguishable from our canonical model. The $p = 0$ case is clearly an extreme scenario, already ruled out by observations of the high metallicity of some GRB hosts (e.g., Levesque et al. 2010c), but its analysis is still useful to highlight the impact of a strong metallicity bias on the GRB host LF.

A scenario where the metallicity bias is absent and the GRB rate traces the star-formation rate is difficult to discriminate from our canonical model based on $z < 1$ observations only, since the two luminosity functions are essentially identical down to the median luminosity of the GRB hosts. The strongest difference between the two scenarios appears instead at $2.5 \lesssim z \lesssim 6$, when the median host luminosities differ by about one magnitude.

This complex situation overall suggests caution when drawing conclusions on metal-bias from a small sample of GRB hosts carrying out a generic comparison with the luminosity and stellar mass functions of star-forming galaxies. For example, Jakobsson et al. (2005) conclude that no metallicity bias is present, but they neglect the dust impact discussed above. When cast in our framework, the GRB host LF determined in that study would instead provide a weak-evidence in favor of the presence of a metallicity bias at a strength broadly consistent with our canonical model. In fact, we would expect that in absence of metallicity bias the GRB-host LF is shallower by $\Delta\alpha \sim 0.2$ at the intermediate redshifts analyzed by

Jakobsson et al. (2005).

3.3. Stellar Masses of GRB hosts

Figure 9 presents the predictions for the stellar masses of GRB hosts based on our model. Qualitatively, the same trends discussed above for the luminosity functions are present and intermediate redshift hosts appear the most promising to discriminate models with different p . This is not surprising, since our model has by construction a one-to-one correspondence between stellar mass and UV luminosity (even though the relation between mass and luminosity changes both with redshift and halo mass because of the evolution of the galaxy assembly time; see Section 2 and Tacchella, Trenti & Carollo 2013; Trenti et al. 2013). Thus, while our model describes well the redshift evolution of the stellar mass density, as well as the flattening at the low-mass end with decreasing redshift, as observed for example by Ilbert et al. (2013), our choice to start from UV luminosity needs to be taken into account in a data model comparison. In fact, this suggests to give more weight to analyses of the star formation rates (UV luminosity), rather than the host mass functions. We stress that this is true in general, and it is not resulting just because we are using a simplified model: The GRB rate traces recent star formation, and not the total stellar mass of the host galaxy. No matter how massive and low-metallicity a galaxy is, if its star formation rate is approaching zero, so will be its GRB rate. Therefore, inference on the metallicity bias based on stellar mass functions, such as that of Boissier et al. (2013), might be affected by higher amount of noise compared to analyses based on star formation rate.

Figure 9 shows that in case of a very strong metallicity bias ($p = 0$), we expect a slight rise in the median stellar mass of the GRB hosts from $z = 0$ to $z \sim 2.5$. Models with weaker or no bias predict instead a steady decrease of the host stellar mass with redshift. When these model predictions are compared against observations (within the caveats discussed above), it is fundamental to take into account sample selection as well, since low-mass hosts may be preferentially missed at high redshift. In addition it is important to ensure modeling consistency as well (e.g. with respect to assumptions on the stellar initial mass function). A preliminary comparison with recent stellar mass measurements (Perley et al. 2013; Hunt et al. 2014) highlights that further modeling and data comparison is needed. In fact, the data, if taken at face value, show an increase of the median stellar mass of GRB hosts with redshift, which would indicate the presence of a strong metal bias in our model. However, the observed stellar masses are generally too high to be consistent with $p \sim 0$, and would rather be suggestive weaker metal bias (plus incompleteness at the low-mass end).

3.4. Metallicity of GRB hosts

Finally, Figure 10 illustrates the model predictions for the metallicity distribution of the GRB hosts. Models with different p have a qualitatively similar trend: host metallicities are expected to decrease with increasing redshift, simply reflecting the underlying mass-metallicity relation that we assume in our model. The detailed choice of p influences the shape of the metallicity distribution, and how rapidly it evolves with redshift. Interestingly, the upper tail (top 5%) of the distribution is very similar in all cases from $p = 0$ to $p = +\infty$, implying that using the maximum metallicity observed for a GRB host bears little insight into the presence, or absence, of a metal-

licity bias. The median, and the lower 20% of the distribution have instead markedly different behaviors, which should make it viable to differentiate between models. For example there is a factor 10 difference in the value of the bottom 20% of the metallicity distribution going from $p = 0$ to $p = +\infty$ at $z = 0$, with the relative difference in metallicity remaining almost unchanged at high- z .

The predictions for the metallicity of the GRB hosts have a direct dependence on the assumed relation between stellar-mass/star formation rate and galaxy metallicity. As discussed in Section 2, we use the redshift-dependent mass-metallicity relation of Maiolino et al. (2008). An alternative possibility would have been to implement the fundamental relation observed at $z \lesssim 2.5$ by Mannucci et al. (2010) which links all three quantities together without introducing any redshift dependence (at least in the redshift range considered by the authors). In Figure 11 we compare the metallicity as a function of star formation rate predicted in our model considering the two relations. It is very interesting, and reassuring, to note that at low redshift ($z = 0.25$ shown in the figure), the two different assumptions lead essentially to the same relation. As the redshift increases, there is however a marked difference: the Mannucci et al. (2010) fit remains at fairly high metallicity, while with the Maiolino et al. (2008) relation, we predict values that are lower by ~ 0.5 dex for high star formation rates (massive and luminous galaxies), with the difference growing significantly for lower star formation rates. Taken at face value, the Mannucci et al. (2010) relation is inconsistent with the observations of low metallicities ($Z \sim 10^{-2} Z_{\odot}$) in GRB-DLAs at $z \sim 2$ which are reported by Cucchiara et al. (2014), since it only predicts $Z \gtrsim 10^{-1} Z_{\odot}$. In addition, it is not clear how to extrapolate the relation above $z > 2.5$, since galaxies at higher redshift start showing systematic deviations, as Mannucci et al. (2010) highlight in their Figure 4 (right panel). While these issues prevent us from implementing an analysis of GRB host observations with the Mannucci et al. (2010) relation, our Figure 11 may suggest that the extrapolation of the mass-metallicity relation by Maiolino et al. (2008) is too steep for faint galaxies, possibly introducing systematic uncertainty in our analysis, which could be evaluated if large complete samples of GRBs metallicity measurements/limits were available.

4. A FIRST APPLICATION TO GRB HOST OBSERVATIONS

4.1. Star Formation Rates

For a proper comparison between model and data, it is fundamental to resort to complete and unbiased samples of follow-up observations. Otherwise, systematics that are hard or even impossible to quantify might affect the inferences obtained. For example, it is likely to expect that observations of GRB hosts with short observations leading to non-detections might be preferentially non reported in the literature compared to a detection of a bright host. This would lead to a luminosity function that is skewed toward higher number density at the bright end, masking the presence of a metallicity bias. Furthermore, dusty hosts might be preferentially missed, and a high dust content might even compromise the success in obtaining a redshift for the GRB from the afterglow, leading in this case to an over-estimation of the impact of the metallicity bias. A complete sample free of selection effects is therefore fundamental.

This is the reason why we consider data from the optically unbiased GRB host (TOUGH) survey (Hjorth et al. 2012) to

illustrate the potential of a comprehensive data-model comparison as a tool to infer the presence and strength of a metallicity bias in GRB production, and to test the inference derived from modeling of the GRB comoving rate. Specifically, we restrict to the *complete* sub-sample presented in Michałowski et al. (2012), which includes UV-inferred star formation rate (uncorrected for dust) for all hosts and which we overplot to our predictions in Figure 8, which are also referring to *observed* UV luminosity therefore providing an uncorrected star formation rate. Despite the low number of points (11 hosts) and their relatively low redshift ($z \lesssim 1.1$), the analysis of the observations provides a first constraint on p independent of the global GRB rate modeling. We carried out a Maximum Likelihood analysis of the star formation rates from Michałowski et al. (2012) at varying p , and show the results in Figure 4 (green line). The likelihood strongly excludes $p = 0$ and has a peak at $p = 0.04$. Unsurprisingly, based on the considerations of Section 3, there is a near-plateau of high likelihood values at $p \gtrsim 0.04$: At 68% confidence, $0.01 < p < 0.12$, but the interval is broader and highly asymmetric for the 90% confidence region, with allowed values $0.1 < p < 0.8$. This is the consequence of the limited discriminating power of a low- z sample. Yet, despite the large uncertainty, it is re-assuring to see that p values inferred independently from the UV luminosity modeling and from the rate modeling (red solid) agree at the $\sim 1.5\sigma$ level. When the two likelihoods are combined together (blue solid), $p \sim 0.2$ remains the most likely solution. This is essentially because a small sample of 11 datapoints is not competitive against the larger amount of information encoded in the comoving GRB rate, derived from all the known events. A plateau value $p \sim 0.2$ implies a probability $p/(1+p) \sim 0.15$ for GRBs to be produced by metal-independent progenitors *in the limit of very low metallicity*, while the actual fraction of GRBs originating from the two channels as a function of redshift is shown in Figure 5.

4.2. Metallicity Distribution

Observations of hosts metallicities can provide a further test to validate/reject the modeling outcome (which we show in Figure 10) for different values of the efficiency parameter p . Unfortunately, and unlike the case for UV luminosity, data are not available for a *complete* sample, complicating a formal likelihood analysis.

Still, a qualitative comparison with results from the compilation of GRB hosts with measured metallicities carried out by Savaglio (2013), and the new recent measurement/re-analysis by Cucchiara et al. (2014) yields good insight: Our canonical model ($p = 0.2$, red lines in figure 10) predicts hosts metallicities that are too high compared to the observed values at low redshift (green points in the figure).

Values $p \lesssim 0.04$ would be needed to improve consistency with these data, pointing toward a lower efficiency of the metal-independent production channel, and thus a stronger presence of the metallicity bias, which has been argued by several studies in this redshift range (Savaglio et al. 2009; Castro-Cerón et al. 2010; Perley et al. 2013), and also derived by our maximum likelihood analysis of the TOUGH host galaxy luminosity (green curve in Figure 4). However, this in turn creates tension with the global modeling of the GRB rate, which prefers $p \gtrsim 0.1$ at 90% confidence.

Of course, this inference on p from host metallicity is valid only under the assumption that the observations we consider have a distribution that is representative of that of a complete

sample. This is complicated because of the difficulty of measuring metallicities for GRB hosts both at the high end (e.g. because of possible dust biases), and at the low end (since hosts are intrinsically faint). The impact of observational biases in the likelihood analysis is clearly seen by analyzing subsamples of the measurements and upper limits on metallicity reported by Cucchiara et al. (2014), and shown as blue points in Figure 10. If we restrict the likelihood analysis at $z \lesssim 3.5$ we have a good agreement between data and our canonical model, with $p = 0.2$ providing a solution within the 68% confidence interval (see magenta line in Figure 4). However, inclusion of all data shifts the likelihood toward significantly higher p values and absence of metallicity bias would be the preferred solution (see red line in Figure 12). This possibly originates because $z > 3.5$ spectroscopic observations have been carried out primarily at low-resolution, which provide lower limits to metallicity (Cucchiara et al. 2014). On the other hand, if one restricts the sample only to high-resolution spectroscopy, then the likelihood analysis yields the opposite result, namely a preference for $p = 0$ (blue line in Figure 12). Still, even assuming this likelihood, when combined with the result from GRB rate modeling, the total analysis shifts only marginally away from our canonical $p = 0.2$ model which remains within the combined 68% confidence interval (black line in Figure 12).

For future progress, it would be extremely helpful to build an observational sub-sample with uniform coverage which is complete and similar to the TOUGH dataset of star-formation rates considered by Michałowski et al. (2012), but targeted at higher redshifts, in order to obtain likelihood constraints comparable or even stronger than those inferred from rate modeling. For this, host follow-up of all GRBs presented by Salvaterra et al. (2012) would be ideal and could solve the tension between the metallicity predictions which favor low p , and the comoving GRB rate modeling which seems to favor higher p .

5. CONCLUSIONS

In this paper we have used a minimal but successful model for the redshift evolution of the luminosity function of star forming (Lyman Break) galaxies to investigate production of long-duration GRBs and properties of their host galaxies. We followed the framework introduced in our earlier works on the connection between GRBs and LBGs as complementary probes of star formation across cosmic time (Trenti et al. 2012, 2013). Here, we have made predictions for the luminosity, stellar mass functions, and metallicity distribution of GRB hosts, depending on the presence and strength of the GRB metallicity bias. The key findings of our modeling, introduced in Sections 2-3 and discussed in Section 4, are the following:

- The luminosity function of GRB hosts is connected to that of star forming galaxies, but changes in the shape are introduced by several factors. First, GRBs trace star formation, therefore to first order UV-bright hosts are preferred, with an approximate scaling given by host luminosity ($\Phi_{(GRB)} \propto \Phi_{(LBG)} \times L$). The presence of a metallicity bias qualitatively counteracts, at least partially, this luminosity function flattening, making GRBs more likely to have faint hosts. This established picture is however missing one key ingredient, which we discussed and modeled, namely the impact of dust reddening. Since dust is proportional to metallicity, and dust masks star formation, we highlight that to first approx-

imation the dust has an impact on the GRB host luminosity function that is comparable but opposite to that of a mild metallicity bias (Figure 7). Analysis of GRB host observations need to take that into account properly or else they would risk to draw (partially) incorrect information on the strength of the GRB metallicity bias.

- The maximum likelihood model derived from analysis of the observed comoving GRB rate is one that has a moderate metallicity bias, with about 80% of GRBs in a very low metallicity environment produced by collapsars and the remaining 20% by a metal-independent channel (such as, e.g. binaries or magnetar engines; see also Jimenez & Piran 2013). However, this model predicts that the large majority of $z \lesssim 1$ GRBs are produced by the metal independent channel, because low- z hosts have metallicities where there is a preferential suppression of collapsars (Figure 5). At intermediate redshifts ($z \sim 3$) the two channels produce comparable numbers of bursts, offering the most discriminating power between alternative scenarios. Finally, at $z \gtrsim 5$ most of the GRBs are produced in metal poor environments where collapsar efficiency has plateaued, so it becomes again hard to discriminate among models with different p .
- We make detailed predictions for the luminosity and stellar mass functions of GRB hosts, as illustrated in the key Figures 8-9. Because of the direct relation between UV luminosity and GRB production, a comparison with luminosity/star formation rates of host galaxies is recommended over the use of stellar masses which are only indirectly, and approximatively, linked to recent star formation. To avoid introducing uncontrolled systematic errors (such as preferential reporting of detections over null results), it is also fundamental to use only complete samples of GRB hosts free of selection effects.
- As a first comparison with observations, we present a maximum likelihood analysis of the star formation rates of the complete sub-sample of TOUGH observations of GRB hosts by Michałowski et al. (2012). The sample size is small (11 hosts) and at low redshift, but nevertheless it provides a preliminary characterization of the metallicity bias from host studies using our framework. The inferred strength of the metallicity bias is lower ($p = 0.04$) but consistent with that of our canonical model within uncertainties, leading to a combined constraint $0.1 < p < 0.35$ at 90% confidence. This means that both the strong metal bias ($p = 0$) and the no bias scenarios ($p = +\infty$) are clearly ruled out.
- Our model predicts the metallicity distribution of GRB hosts as well. This is shown in Figure 10, which highlights that characterizing the median (and the lower 50%) of the metallicity distribution of GRB hosts seems to be a powerful indicator of the strength of the metallicity bias. In contrast, the top of the metallicity of GRB hosts is remarkably similar among different models, providing relatively little insight to constrain p . The predictions shown in Figure 10 for $p = 0.2$ appear in conflict with the low-redshift observations of GRB host metallicities by Savaglio et al. (2009). This suggests that smaller p values smaller or closer to the peak of the likelihood from GRB host luminosities at $p = 0.04$

yield an overall better description of the observations. However, we can make this statement only in a qualitative sense, since we do not have a complete sample of GRB host metallicities, and observational effects can strongly affect a formal maximum likelihood analysis, as shown in Figure 12.

These conclusions allow us to address the two questions we posed in Section 1 as one of the motivations to our study: Are GRBs more probable in low-metallicity environments compared to higher metallicity? Is there a maximum metallicity cut-off? We conclude that there is clear evidence for a metal-dependent relation between GRB and star-formation rate, with low metallicity environments preferentially producing bursts (see also Jimenez & Piran 2013). However, a sharp metallicity cut-off is strongly ruled out by the data-model comparison. At the current time, the main limitation of the analysis we presented is given by the lack of a well defined complete sample of GRB host observations at intermediate redshifts. This should be the top priority for further progress in the characterization of the physics of GRB explosions from studies of their host galaxies.

Because our canonical model parameter $p = 0.2$, inferred primarily from the GRB rate modeling, appears in tension with metallicity measurements, it is important to focus on acquiring more data on star formation rates and metallicities of GRB hosts. Future observations should also be able to test directly model consistency, namely the three main in-

gredients we used to construct predictions: (1) calibration of the luminosity functions starting from LBG observations; (2) empirical, observationally motivated relations for metallicity versus mass/luminosity (with its extrapolation to fainter than observed galaxies) and for dust content of GRB hosts; (3) GRB efficiency versus metallicity described by a simple relation with one free parameter (p). For example, ALMA observations of GRB hosts have the potential to characterize star formation rates, and measure directly dust and metal content from molecular line diagnostic, bypassing the dust absorption modeling present in the current work focused on rest-frame UV data. Finally, in a few years, 30m class observatories from the ground, and the *James Webb Space Telescope*, will not only be capable of detecting fainter hosts than those seen with current facilities, but also provide spectra of the hosts seen today, thereby measuring directly the metallicity distribution of the environments in which GRBs explode.

We thank Sandra Savaglio for useful discussions, Nino Cucchiara for sharing data, and an anonymous referee for helpful comments. This work was partially supported by the European Commission through the Marie Curie Career Integration Fellowship PCIG12-GA-2012-333749 (MT) and by NSF Grant No. AST 1009396 (RP). RJ acknowledges support from Mineco grant FPA2011-29678-C02-02. Tabulated model predictions are available in electronic format.

REFERENCES

- Alavi, A., Siana, B., Richard, J. et al. 2013, ApJ, submitted, arXiv:1305.2413
- Behroozi, P. S., Wechsler, R. H., & Conroy, C. 2013, ApJ, 762, 31
- Berger, E., Cowie, L. L., Kulkarni, S. R., et al. 2003, ApJ, 588, 99
- Berger, E., Fox, D. B., Kulkarni, S. R., Frail, D. A., Djorgovski, S. G. 2007, ApJ, 660, 504
- Berger, E., Chornock, R., Holmes, T. R., et al. 2011, ApJ, 743, 204
- Bloom, J. S., Kulkarni, S. R., and Djorgovski, S. G., 2002, AJ, 123, 1111
- Boissier et al. 2013, A&A, 557, 34
- Bouwens, R. J., Illingworth, G. D., Franx, M. & Ford, H. 2007, ApJ, 670, 928
- Bouwens, R. J., Illingworth, G. D., Oesch, P. A. et al. 2011, ApJ, 737, 90
- Bouwens, R. J. et al., 2014, ApJ, submitted, arXiv:1306.2950
- Bouwens, R. J. et al., 2014, ApJ, submitted, arXiv:1403.4295
- Bradley, L. D., Trenti, M., Oesch, P. A., et al. 2012, ApJ, 760, 108
- Bruzual, G., & Charlot, S. 2003, MNRAS, 344, 1000-1028
- Cantiello, M., Yoon, S.-C., Langer, N., Livio, M. 2007, A&A, 465L, 29
- Castro-Cerón, J. M. et al. 2010, ApJ, 721, 1919
- Chary, R., Berger, E. and Cowie, L. 2007, ApJ, 671, 272
- Cucchiara, A. et al. 2011, ApJ, 736, 1
- Cucchiara, A. et al. 2014, arXiv:1408.3578
- Elliott, J., Krühler, T., Greiner, J. et al. 2013, A&A, submitted, arXiv:1306.0892
- Ellis R. S. et al. 2013, ApJ, 763, 7
- Fruchter, A. S., Thorsett, S. E., Metzger, M. R. et al. 1999, ApJ, 519, 13
- Fruchter, A. S. et al. 2006, Nature, 441, 463
- Finlator, K., Oppenheimer, B. D. & Davé, R. 2011, MNRAS, 410, 1703
- Fynbo, J. P. U. et al. 2003, A&A, 406, 63
- Fynbo, J. P. U. et al. 2008, ApJ, 683, 321
- Fryer, C. L. & Heger, A. 2005, A&A, 406, L63
- Galama, T. J., Vreeswijk, P. M., van Paradijs, J. et al. 1998, Nature, 395, 670
- Graham, J. F. & Fruchter, A. S. 2013, ApJ, 774, 119
- Greiner, J., Krühler, T., Klose, S. et al. 2011, A&A, 526, A30
- Hao, J. & Yuan, Y. 2013, ApJ, accepted, arXiv:1305.5165
- Hjorth, J., Sollerman, J., Møller, P., et al. 2003, Nature, 423, 847
- Hjorth, J., Malesani, D., Jakobsson, P. et al. 2012, ApJ, 756, 187
- Hopkins, A. M. & Beacom, J. E., ApJ, 651, 142
- Hunt, L. K. et al. 2014, A&A in press
- Ilbert, O. et al. 2013, A&A, 556, 51
- Jakobsson P. et al. 2005, MNRAS, 362, 245
- Jimenez R., Piran T., 2013, ApJ, 773, 126
- Kistler, M. D., Yüksel, H., Beacom, J. F. et al. 2009, ApJ, 705, L104
- Kewley, L. J. and Dopita, M. A. 2002, ApJS, 142, 35
- Kewley, L. J., Brown, W. R., Geller, M. J., Kenyon, S. J., Kurtz, M. J. 2007, AJ, 133, 882
- Kewley, L. J. and Ellison, S. L. 2008, ApJ, 681, 1183
- Kohn, S. A. et al. 2015, arXiv:1501.01004
- Laskar, T., Berger, E. & Chary, R. 2011, ApJ, 739, 1
- Lacey, C., & Cole, S. 1993, MNRAS, 262, 627-649
- Levesque, E. M. et al. 2010a, AJ, 140, 1557
- Levesque, E. M., Soderberg, A. M., Kewley, L. J. & Berger, E. 2010, ApJ, 725, 1337
- Levesque, E. M., Kewley, L. J., Graham, J. F., Fruchter, A. S., 2010, ApJ, 712, 26
- Levesque E. M. 2014, PASP, 126, 1
- Lunnan, R. et al. 2014, ApJ, 787, 138
- MacFadyen, A. I., Woosley, S. E. 1999, ApJ, 524, 262
- Madau, P., Pozzetti, L., & Dickinson, M. 1998, ApJ, 498, 106
- Maiolino, R., Nagao, T., Grazian, A. et al. 2008, A&A, 488, 463
- Mannucci, F. et al. 2010, MNRAS, 408, 2115
- MacFadyen, A. I. & Woosley, S. E. 1999, ApJ, 524, 262
- McLure, R. J., Dunlop, J. S., Bowler, R. A. A., et al. 2013, MNRAS, in press, arXiv:1212.5222
- Metzger, B. D., Giannios, D., Thompson, T. A., Bucciantini, N., Quataert, E. 2011, MNRAS, 413, 2031
- Meurer, G. R., et al. ApJ, 521, 64-80
- Michałowski, M. J. et al. 2012, ApJ, 755, 85
- Modjaz, M., Kewley, L., Kirshner, R. P. et al. 2008, AJ, 135, 1136
- Modjaz, M. et al. 2008, ApJ, 645, L21
- Nuza, S. E. et al. 2007, MNRAS, 375, 665
- Ouchi, M., Shimasaku, K., Furusawa, H., et al. 2010, ApJ, 723, 869
- Panther B., Heavens A. F., Jimenez R., 2003, MNRAS, 343, 1145
- Panther B., Jimenez R., Heavens A. F., Charlot S., 2008, MNRAS, 391, 1117
- Perley, D. A., Cenko, S. B., Bloom, J. S. et al. 2009, AJ, 138, 1690
- Perley, D. A., Levan, A. J., Tanvir, N. R. et al. 2013, ApJ, submitted, arXiv:1301.5903
- Perna, R., Duffell, P., Cantiello, M., MacFadyen, A. I. 2014, ApJ, 781, 119
- Planck Collaboration 2013, arXiv:1303.5076
- Podsiadlowski, P., Ivanova, N., Justman, S. & Rappaport, S., 2010, MNRAS, 406, 840

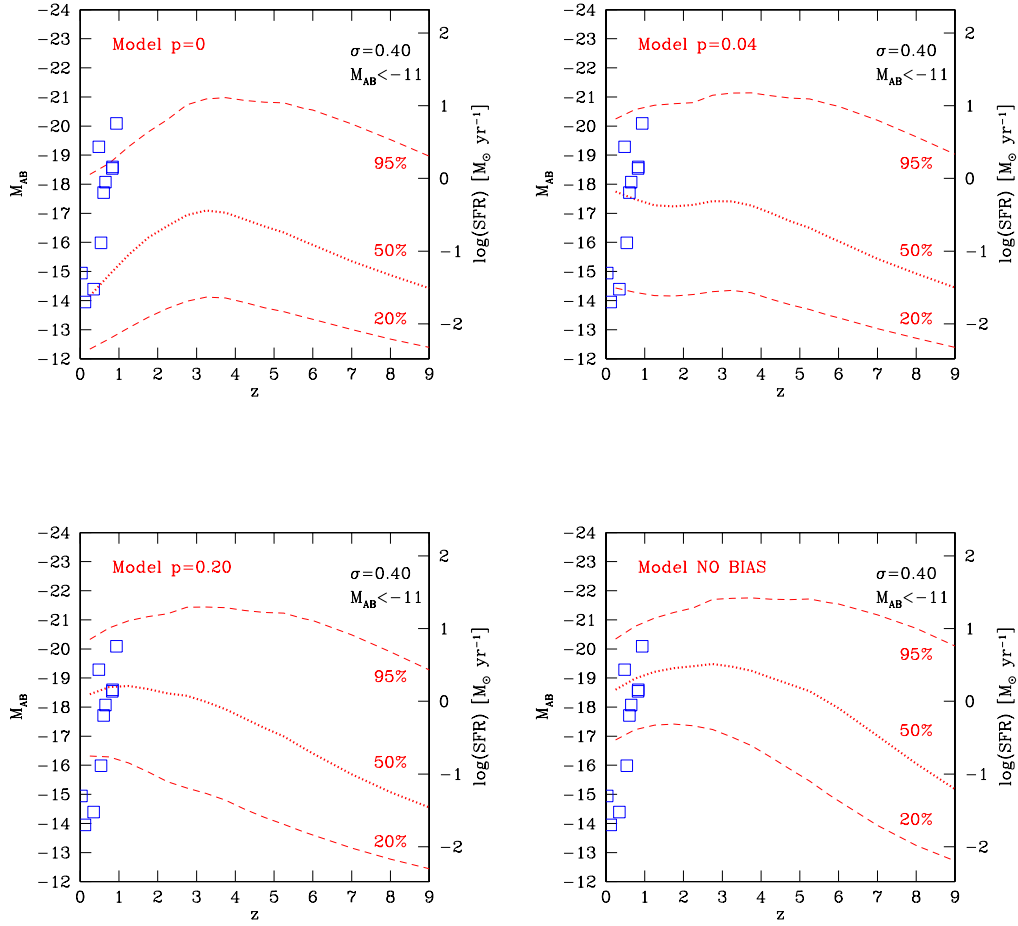


FIG. 8. — Evolution of the upper 95% (top dashed), median (bold dotted) and lower 20% (bottom dashed) of the luminosity function (including dust reddening) of GRB host galaxies, with each panel showing model predictions for different efficiencies of the metal-independent channel for GRB production. Increasing values of p are presented from top-left to bottom-right, from strong metal-dependence ($p = 0$, top left) to absence of metal bias ($p = +\infty$, bottom right). Our canonical model $p = 0.2$ is shown in the bottom left. For each panel, the AB magnitude (restframe UV at 1600 Å) is translated into a star formation rate on the right vertical axis, following Madau et al. (1998). Data from the *complete* TOUGH sub-sample of Michałowski et al. (2012) are shown as blue open squares.

Pontzen, A. et al., 2010, MNRAS, 402, 1523
 Prochaska, J. X., et al. 2004, ApJ, 611, 200
 Robertson, B. E. & Ellis, R. S. 2012, ApJ, 744, 95
 Robertson, B. E., Furlanetto, S. R., Schneider, E. et al., 2013, ApJ, 768, 71
 Salvaterra, R. et al. 2009, Nature, 461, 1258
 Salvaterra, R. et al. 2013, ApJ, 749, 68
 Salvaterra, R. et al. 2013, MNRAS, 429, 2718
 Savaglio, S., Glazebrook, K. & Le Borgne, D. 2009, ApJ, 691, 182
 Savaglio, S., Rau, A., Greiner, J. et al. 2012, MNRAS, 420, 627
 Savaglio, S. 2013, EAS Publications Series, 61, 381
 Schmidt, K. B., Treu, T., Trenti, M. et al. 2014, ApJ, 786, 57
 Schechter, P. 1976, ApJ, 203, 297
 Sheth, R. K., & Tormen, G. 1999, MNRAS, 308, 119-126
 Shimasaku, K., Kashikawa, N., Doi, M., et al. 2006, PASJ, 58, 313
 Stanek, K. Z., Gnedin, O. Y., Beacom, J. F. et al. 2006, Acta Astronomica, 56, 333
 Svensson, K. M., Levan, A. J., Tanvir, N. R., et al. 2010, MNRAS, 505, 47
 Smit, R., Bouwens, R. J., Franx, M., et al. 2012, ApJ, 756, 14

Tacchella, S., Trenti, M. & Carollo, C. M. 2013, ApJ, 768, 37 [TCC13]
 Tanvir, N. R., Fox, D. B., Levan, A. J. et al. 2009, Nature, 461, 1254
 Tanvir, N. R., Levan, A. J., Fruchter, A. S. et al. 2012, ApJ, 754, 46
 Thoene, C. C., Greiner, J., Savaglio, S., & Jehin, E. 2007, ApJ, 671, 628
 Tojeiro R., Heavens A. F., Jimenez R., Panter B., 2007, MNRAS, 381, 1252
 Trenti, M., Stiavelli, M. & Shull, J. M. 2009, ApJ, 700, 1672
 Trenti, M., Stiavelli, M., Bouwens, R. J. et al. 2010, ApJ, 714, L202
 Trenti, M., Bradley, L. D., Stiavelli, M. et al. 2011, ApJ, 727, L39
 Trenti, M., Perna, R., Levesque, E. M. et al. 2012, ApJL, 749, 38
 Trenti, M., Perna, R., Tacchella, S. 2012, ApJL, 773, 22
 Virgili, F. J., Zhang, B., Nagamine, K. & Choi, J. 2011, MNRAS, 417, 3025
 Wanderman, D. and Piran, T. 2010, MNRAS, 406, 1944
 Wang, F. Y. and Dai Z. G. 2014, arXiv:1406.0568
 Woosley, S. E. 1993, ApJ, 405, 273
 Woosley, S. E. and Heger, A. 2006, ApJ, 637, 914
 Yoon, S. C., Langer, N. & Norman, C. 2006, A&A, 460, 199

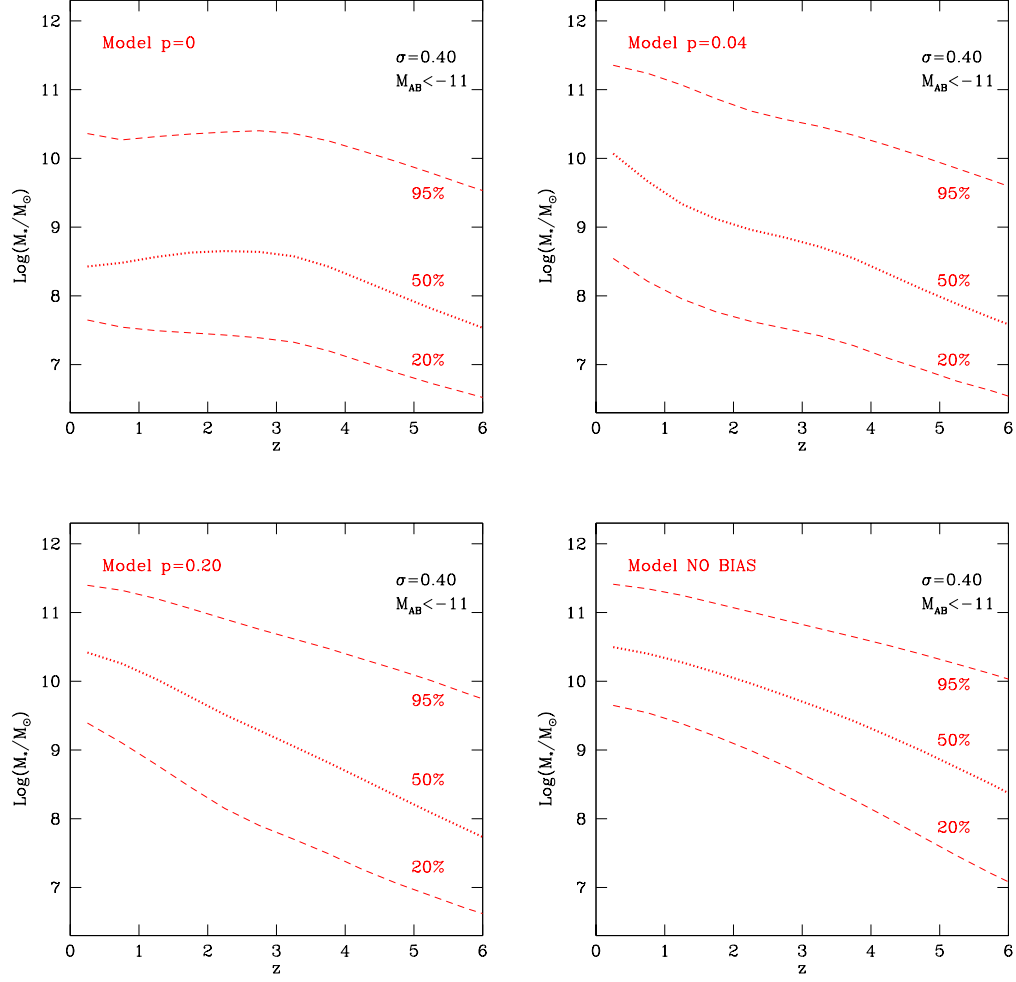


FIG. 9.— Evolution of the upper 95% (top dashed), median (bold dotted) and lower 20% (bottom dashed) of the stellar masses of GRB host galaxies versus redshift. As in Figure 8, each panel shows model predictions for different efficiencies of the metal-independent channel for GRB production.

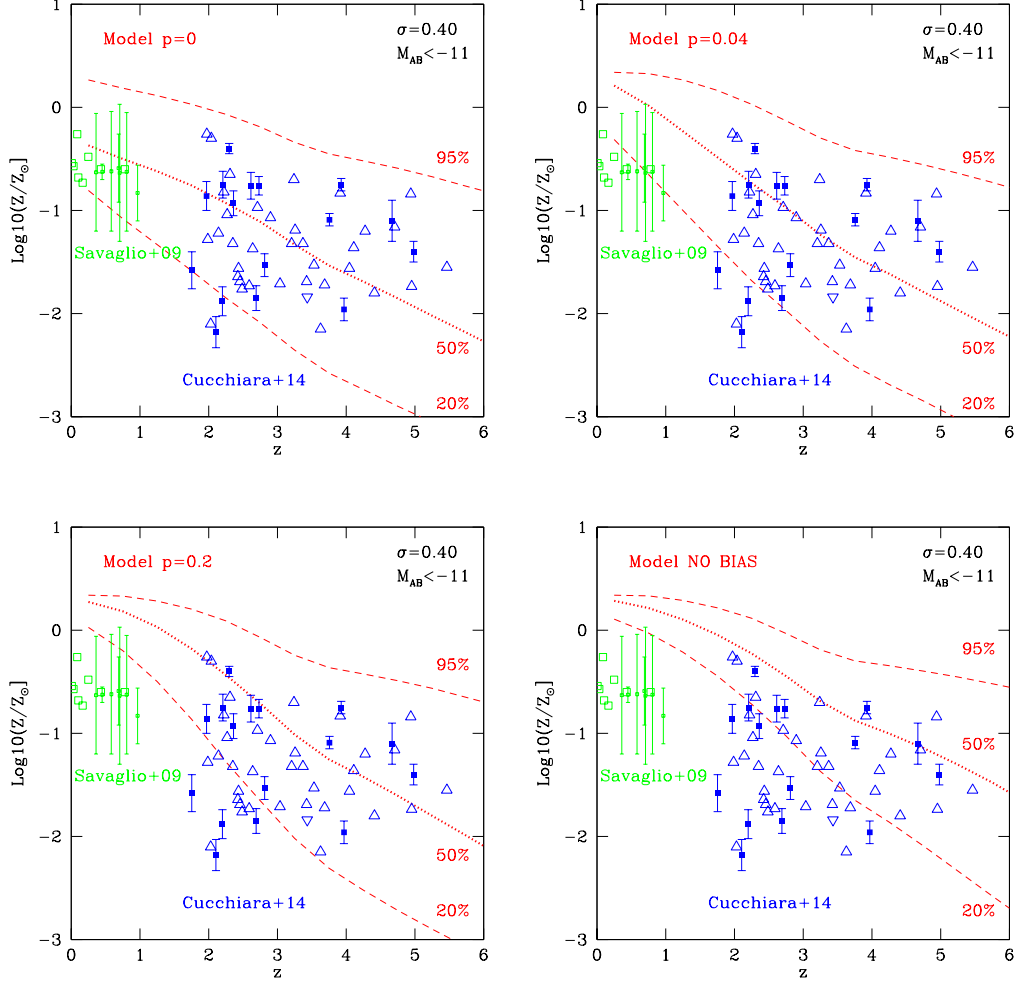


FIG. 10.— Evolution of the upper 95% (top dashed), median (bold dotted) and lower 20% (bottom dashed) of the metallicity (solar units) of GRB host galaxies versus redshift. As in Figures 8-9, each panel shows model predictions for different efficiencies of the metal-independent channel for GRB production. Overplotted we report measurements and lower/upper limits on metallicity from Savaglio et al. (2009) and Cucchiara et al. (2014), although we stress that the samples are not complete, complicating the interpretation of the data-model comparison.

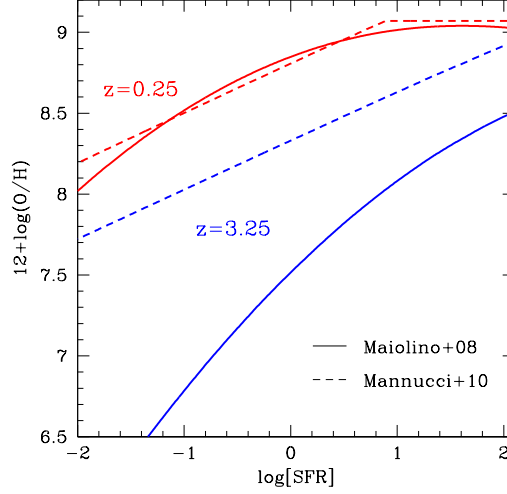


FIG. 11.— Metallicity (in $12 + \log(O/H)$ scale with solar value associated to 8.7) versus star formation rate as inferred through our model using the Maiolino et al. (2008) mass-metallicity relation (solid line) and the Mannucci et al. (2010) mass-metallicity-star-formation-rate relation (dashed line) for two redshifts ($z = 0.25$ in red) and ($z = 3.25$ in blue). The two relations give comparable results at low z but differ systematically at high z .

TABLE 1
SCHECHTER FITS FOR GRB-HOST LF (REST-FRAME UV)

z	$p = 0$		$p = 0.04$		$p = 0.20$		NO BIAS	
	$M_{AB}^{(*)}$	α	$M_{AB}^{(*)}$	α	$M_{AB}^{(*)}$	α	$M_{AB}^{(*)}$	α
0.25	-20.3	-1.2	-19.4	-0.1	-19.4	-0.1	-19.4	-0.1
0.75	-20.2	-1.4	-19.8	-0.3	-19.7	-0.1	-19.7	-0.1
1.25	-20.1	-1.3	-20.1	-0.5	-20.0	-0.2	-20.0	-0.1
1.75	-20.2	-1.1	-20.3	-0.6	-20.2	-0.3	-20.2	-0.1
2.25	-20.3	-0.9	-20.5	-0.7	-20.5	-0.4	-20.4	-0.2
2.75	-20.7	-0.8	-20.9	-0.8	-20.9	-0.6	-20.9	-0.4
3.25	-20.9	-0.8	-21.0	-0.8	-21.0	-0.7	-21.0	-0.5
3.75	-21.0	-0.9	-21.1	-0.8	-21.1	-0.7	-21.1	-0.5
4.25	-21.0	-0.9	-21.1	-0.9	-21.2	-0.8	-21.1	-0.6
4.75	-21.1	-1.0	-21.2	-0.9	-21.3	-0.8	-21.2	-0.6
5.25	-21.3	-1.0	-21.3	-1.0	-21.4	-0.9	-21.4	-0.7
5.75	-21.3	-1.1	-21.3	-1.1	-21.4	-1.0	-21.4	-0.8
6.00	-21.3	-1.1	-21.3	-1.1	-21.4	-1.0	-21.4	-0.8
7.00	-21.3	-1.2	-21.3	-1.2	-21.4	-1.1	-21.3	-0.9
8.00	-21.2	-1.3	-21.2	-1.3	-21.3	-1.2	-21.3	-1.0
9.00	-21.1	-1.5	-21.2	-1.4	-21.2	-1.4	-21.2	-1.2

^a The Schechter fit parameters provided above for models with different p value are valid in the interval $-22 < M_{AB} < -17.5$. At fainter magnitudes the GRB host LF may exhibit significant differences, especially at low redshift where it becomes steeper.

TABLE 2
MODEL PREDICTIONS FOR GRB HOST PROPERTIES

z	p	$\text{Mag}_{UV}^{(w/dust)}$	Mag_{UV}	M_*	M_{DM}	$\log_{10}(Z/Z_{\odot})$	#
3.75	0.2	-2.391e+01	-2.633e+01	4.566e+11	9.682e+13	-1.462e-02	2.564e-08
3.75	0.2	-2.389e+01	-2.630e+01	4.451e+11	9.527e+13	-1.673e-02	3.996e-08
3.75	0.2	-2.386e+01	-2.626e+01	4.301e+11	9.375e+13	-1.962e-02	6.403e-08
3.75	0.2	-2.384e+01	-2.623e+01	4.193e+11	9.224e+13	-2.177e-02	8.609e-08
3.75	0.2	-2.382e+01	-2.620e+01	4.106e+11	9.077e+13	-2.358e-02	1.105e-07

NOTE. — Table 2 is published in its entirety in the electronic edition of the *Astrophysical Journal*. A portion is shown here for guidance regarding its form and content.

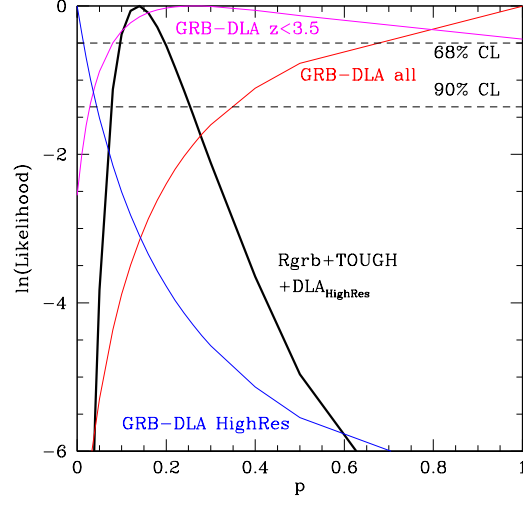


FIG. 12.— Likelihood for the value of the metal-independent channel for GRB production (p), derived from analysis of the metallicity of GRB-DLAs, using data from Cucchiara et al. (2014). The red line shows the result from analysis of the full sample; the magenta line for the subsample of $z < 3.5$ data, while the blue line is for the subsample of high-resolution data. The black solid line shows the combined likelihood when adding comoving GRB rate and TOUGH star formation rate constraints to the subsample of high-resolution data. Dashed horizontal lines denotes the likelihood boundaries at 68% and 90% confidence. Compared to Figure 4, which included both high and low resolution data at $z < 3.5$, the combined likelihood contours obtained using high-resolution data (black line) are slightly shifted toward smaller p .